Experimental investigations on hot forming of AA6082 using advanced plasma nitrocarburised and CAPVD WC: C coated tools

Dong, Yangchun; Zheng, Kailun; Fernandez, Jonathan; Li, Xiaoying; Dong, Hanshan; Lin, Jianguo

DOI:
10.1016/j.jmatprotec.2016.09.023

Document Version
Peer reviewed version

Citation for published version (Harvard):
Dong, Y, Zheng, K, Fernandez, J, Li, X, Dong, H & Lin, J 2017, 'Experimental investigations on hot forming of AA6082 using advanced plasma nitrocarburised and CAPVD WC: C coated tools', *Journal of Materials Processing Technology*, vol. 240, pp. 190-199. https://doi.org/10.1016/j.jmatprotec.2016.09.023

Title: Experimental investigations on hot forming of AA6082 using advanced plasma nitrocarburised and CAPVD WC: C coated tools

Author: Yangchun Dong Kailun Zheng Jonathan Fernandez Xiaoying Li Hanshan Dong Jianguo Lin

PII: S0924-0136(16)30343-0
DOI: http://dx.doi.org/doi:10.1016/j.jmatprotec.2016.09.023
Reference: PROTEC 14972

To appear in: *Journal of Materials Processing Technology*

Received date: 26-4-2016
Revised date: 20-9-2016
Accepted date: 24-9-2016

Please cite this article as: Dong, Yangchun, Zheng, Kailun, Fernandez, Jonathan, Li, Xiaoying, Dong, Hanshan, Lin, Jianguo, Experimental investigations on hot forming of AA6082 using advanced plasma nitrocarburised and CAPVD WC: C coated tools.Journal of Materials Processing Technology http://dx.doi.org/10.1016/j.jmatprotec.2016.09.023

Experimental investigations on hot forming of AA6082 using advanced plasma nitrocarburised and CAPVD WC: C coated tools

Yangchun Dong[1,1], Kailun Zheng[2], Jonathan Fernandez[3], Xiaoying Li[1], Hanshan Dong[1], and Jianguo Lin[2]

[1] School of Metallurgy and Materials, University of Birmingham, B15 2TT Birmingham, UK

[2] Department of Mechanical Engineering, Imperial College London, SW7 2AZ London, UK

[3] AIN Asociación de la Industria Navarra, 31191 Navarre, Spain

Highlights

- Bespoke stamping test rig to validate the tribological performances of lubricated and dry forming tools
- Innovative plasma and CAPVD treatments aiming for lubricant-free hot forming of AA6082
- Observation and quantifying the adhesion of aluminium during stamping

Abstract The use of lubricant for hot stamping process of sheet material can reduce the tendency of adhesion between work-piece and tool significantly and the friction coefficient. However, the post-process of cleaning the formed part and lubricating the tools before each stamping operation can compromise the manufacturing efficiency. It is especially challenging for hot stamping because reducing lubricant could lead to severe adhesion between tool and blank during stamping. Hence, it is desirable to develop an advanced tooling technique suitable for hot stamping processes of aluminium alloys. In this paper, an innovative tooling technology enabling hot and cold forming of aluminium with little lubricant has been developed using plasma thermochemical treatment and Cathodic Arc Physical Vapour Deposition (CAPVD) technologies. The forming performance was validated on a top-hat part stamping test to benchmark the performance of the developed tools at different forming temperature, blank-holding force (BHF) and lubrication state. The results show that WC: C coating prepared by CAPVD adequately reduced the aluminium sticking on the tool surfaces, to the extent that it achieved an 80% lubricant reduction in the hot forming stamping of a top-hat part with a drawing depth of

[1] Corresponding author : yangchun.dg@gmail.com

70 mm. The morphology of die showed that aluminium adhesion at the corner area of the die where the contact pressure doubled was still noticeable, while no severe adhesion was observed on the top flat surfaces. A further investigation of tribology on hot and cold stage tribometers was deployed to quantify the friction coefficient and wear resistance of tooling materials which were found correlated to the material's universal hardness and time-dependent adhesion rate of aluminium.

Keywords Coatings; Deep draw; Aluminium; Adhesion; Tool wear; Plasma nitriding.

1 Introduction

High strength automotive aluminium alloys such as AA6xxx have been used for light-weight automobile body and chassis structures owing to the advantages of significant fuel saving and gas emission reduction. The poor ductility of the AA6xxx series at room temperature limits the forming of complex-shape components. In recent years, forming processes at elevated temperatures, such as superplastic forming (SPF) and warm forming have been applied to manufacture complex-shape components, however, still with limited material choices and production efficiency. Lin et al. proposed and patented a novel hot stamping process of aluminium alloys which is known as solution Heat treatment, Forming and in-die Quenching (HFQ®). The use of newly developed HFQ® technology has provided a novel forming method to form complex-shaped and high-quality heat treatable aluminium alloy components with high manufacturing efficiency suitable for mass production.

The 'key issue' of hot stamping process of aluminium alloys identified by automotive industry is the tendency of soldering the ductile and highly reactive aluminium to the tool steel. A report by NASA described the phenomena of adhesion at a molecular level (Buckley 1975) and transferring from mono- to multi- layer film according to the electronic nature, surface energies and structural lattice disregistry. Recently, Al-tool soldering was confirmed with in-situ scanning electron microscopy by Heinrichs (Heinrichs et al. 2012). Many researches have shown that adhesion of solid surface involves mechanical anchoring,

absorption and metallic bonding, which might occur spontaneously at the stamping contact surfaces as demonstrated in a postulated model (Fig. 1). To alleviate these problems, aluminium forming requires the application of costly thermal lubricants. However, as suggested in a recent European project report (Laurent 2007), a reduction of the use of lubricants has a meaningful impact to address ecological concerns, which makes raw materials usage sustainable and increases production efficiency. The risk of insufficient lubrication of forming tools can result in defects such as limited material extraction, tool wear and galling. Its effect on the surface quality and roughness of the formed products during lubricant free cold massive forming of aluminium was also mentioned by Wank (Wank et al. 2006). Uda et al. found that the above potential problems can be also found for the hot stamping of Al-coated steel (Uda et al. 2016). In addition, the friction force tested on hot drawing machine rise sharply during dry forming at a very early stage as well as the lubricated conditions at the end of the test. The fracture of die occurring at the punch radius area during dry forming condition was due to the lack of lubrication.

With the aim of improving the tribological performance at the interface between workpiece and tool, a feasible 'green' approach of using coating on tool surface was proposed by Vollertsen et al. (Vollertsen et al. 2015). For example, Hansen et al. reported that many hard coatings, such as chemical vapour deposition (CVD) carbide (TiC) and Toyota coating, have been used to treat steel tool surfaces for the drawing and restrike processes of structural components since the 1980s (Hansen et al. 1986); Surface heat treatment of tool steels, such as oxidation and nitriding, are frequently applied to the steel die surfaces to reduce the tool wear and prolong the tooling lifetime. A suitable tool for the mass production process is a M4 + TiC die that stamped over 10,000 pcs B-Pillar, as suggested by (Mihail et al. 2007), and further optimisation of coating techniques are still required tremendously. To this end, very few studies have been performed on developing coatings suitable for the hot stamping of

aluminium alloys due to the difficulty of producing tooling for the ductile and adhesive aluminium workpiece at high temperature.

Self-lubricating coating is another potential method to decrease the coefficient of friction (CoF) and reduce soldering between the hot workpiece metal and tool. General Motors U.S. used a solid BN film with a thickness of 50 μm on the die to achieve a CoF between 0.15-0.2 (Hanna 2009), and successfully formed AA5083 alloy at 450 °C (Krajewski et al. 2004). Murakawa (Murakawa et al. 1995) investigated the possibility of dry-drawing process of aluminium to a small size cups of 20 mm using diamond-like carbon coated dies. In a recent report by Agarwal (Agarwal et al. 2013), the use of a reactive plasma to produce a nano-C thin film on top of hardened surface in a multi-step process was able to reduce the sliding friction force against dual phase (DP) steels. Quantitative tribological data of machining tools coated with diamond-like-carbon (DLC) for aluminium drilling (Bhowmick et al. 2008) and cutting (Fukui et al. 2004), as well as using them for dry shear-stampings (Dohda et al. 2014) and dry deep drawing (Murakawa et al. 2003) show that the unique combination of lubricity and high hardness of the carbon-based coating might be suitable for the forming tools used for lubricant-free hot stamping process of aluminium alloys.

In this study, gray cast iron was used as the tooling material owing to the low cost compared with conventional hot work tool steel. To overcome the low strength of gray cast iron compared with the hot work tool steel, the gray cast iron can be surface hardened by plasma (Dong et al. 2015) and gas thermochemical treatments (Rolinski 1987). Hence, plasma nitrocarburising of cast iron has been developed to improve the strength and increase the lifetime of forming tools in this study. Based on a previous feasibility study of the self-lubricated tools (Dong et al. 2015), plasma nitriding and plasma nitrocarburising plus CAPVD coatings was selected as the surface engineering process of the die. The performance

of the HFQ® forming technique combined with newly applied coatings on the blank-holder was examined for the first time on a top-hat shaped hot stamping testing rig using a series of controlled forming conditions. The geometry of deep-draw parts and the post-stamping morphology of die surfaces are reported. The particular friction behaviour, wear rate and hardness of tool materials were tested separately to provide a detailed root-cause analysis of the tribological phenomenon between the tooling materials and aluminium alloy.

2 Experimental design

2.1 Test-piece and tool material

Commercial AA6082-T6 condition aluminium sheet (Smiths Metal Centres, UK) with a thickness of 1.5 mm was selected as the test-piece material. The chemical composition of AA6082 is given in Table 1. Rectangular test-pieces were pre-cut by laser cutting to dimensions of 240 mm × 86 mm × 1.5 mm. These test-pieces were stamped using a series of plasma treated and CAPVD coated cast iron tools in both cold and hot stamping conditions. With regard to the cold stamping tests, the AA6082 test-pieces were annealed at 415 °C with a soaking time of one hour and subsequent cooling in the furnace to obtain the 'O' condition (Aginagalde et al. 2009). With regard to the hot stamping tests, AA6082 test-pieces were directly heating up to 430 ℃ with a soaking time of 2 mins prior to hot stamping.

The tool material selected for the top-hat drawing test was pearlitic gray cast iron and cast according to the automotive metric standard NAAMS G3500 (S.C. Plasmaterm S.A., Romania). G3500 has a pearlitic matrix containing uniformly distributed and randomly orientated type #A graphite with the approximate size of 10×100 μm.

2.2 Tooling technique

Cast iron tool material was case-hardened through a low-temperature plasma nitriding (PN) process in a standard DC plasma furnace (Klöckner 40 kW, Germany) using a gas mixture of

75% H_2 + 25% N_2 at a pressure of 4 mbar. The operating temperature was 525 ºC and the soak time was 24 hours. The plasma nitrocarburising (PNC) process parameters have been taken from previous studies (Dong et al. 2015; Roliński et al. 2009) with optimised diffusion thickness. Gas mixture of 50% H_2 + 48% N_2 + 2% CH_4 with a pressure of 1 mbar was used for the PNC process at the temperature of 575 ºC for 4 hours. The surface hardness of treated tools was determined using a nano-indentation (Micro Materials Ltd UK) in accordance with the standard ASTM E92 method. Two groups of carbonaceous CAPVD coating techniques—diamond-like carbon (a-C) and W doped carbon (WC: C)—were developed to pursue the objective of low-friction and anti-sticking performances. Both types were prepared by cathodic arc enhanced PVD and deposited at a temperature range of 200-350 ºC (Asociación de la Industria, Spain). The most appropriate sp3/sp2 hybridisation ratio was developed to achieve a combination of properties with low adhesion, wear life and thermal stability at elevated temperatures.

2.3 Top-hat part forming test

To benchmark performance of tool materials, the above tooling techniques were validated using a top-hat stamping experiment with different lubrication conditions in both cold and hot stamping conditions, of which the results was compared to the industry existing lubrication methods. A target was set to replace the lubricated untreated tool with a surface engineered tool that matches or outperforms the existing tooling technology. The performance of each engineered tooling surface was discussed with the assistance of its corresponding tribological performance tested from separate tribometers. Fig. 2 (a) shows the experimental set-up of the top-hat stamping rig and the forces distributing on the blank and dies during forming. The rectangular punch was fixed on the bottom plate which was supported by a gas cushion system. A pair of detachable inserts including an insert and a blank-holder was mounted on the bottom surfaces of the die for a convenient replacement. Various coatings were prepared

on the right-hand side of the testing rig, while on the left-hand side, a pair of untreated blank-holder and insert was fully lubricated with heat-resistant die lubricant. This branded lubricant was confirmed containing solid graphite by Raman spectral using 488.0 nm lines of argon-iron lasers. The entire test-rig were mounted on a hydraulic press with the maximum forming speed of 600 mm/s and a total stroke of 70 mm under the maximum load of 1 MN. The controlled parameters of stamping process and the geometry of dies were given in Table. 2.

The procedure of hot stamping consisted of four stages of tool motion: gravity, holding, stamping and quenching as shown in Fig. 3. After heating of the T6 test-piece to a target temperature of 430 °C and soaked for 2 mins. The hot test-piece was quickly transferred on top of the blank-holders within 7-10 s to minimise temperature loss. Upon the activation of the hydraulic press, the ram moved downwards to close the gap between die and blank-holders. The blank-holding force was supplied via the blank-holding force bars attached to the mechanical gas springs. In the stamping stage, the die moved further downwards and the test-piece was deformed according to the punch and die profile. Once the formed part had quenched to room temperature, the die moved upwards and released the deformed parts. During each test, the left-hand side blank-holder was re-lubricated, while the right-hand blank-holder was replaced with a range of tools and lubrication conditions.

In order to quantify the performance of the surface engineered tools, the geometries of formed top-hat part was measured as shown in Fig. 4. A flange length L_x is defined as the distance between the flange edge and the edge of the radius on the formed part. As there may be a variation of flange length through the depth of the part due to the flatness error of machining, the average value of flange lengths between the front and the back was measured, as shown in Fig. 4. L_{left} is the average flange length of the formed part formed by the reference side blank-holder, whereas L_{right} corresponding to the test side. A ratio of the

lengths of two flange regions is presented in Eq. (1), which is defined as the flange ratio ζ. It is assumed that a higher friction coefficient at the interfaces between test side dies and test-pieces would cause a greater remaining flange length on the test side and a subsequent smaller length ratio ζ.

$$\zeta = L_{left}/L_{right} \quad (1)$$

2.4 Tribological test

The tribological performances tested using reciprocating and pin-on-disc tribometers were deployed to investigate the coefficient of friction and wear of tooling materials as related to the adhesion of aluminium. The testing conditions were set the same with that of its top-hat forming conditions for the purpose of comparison with the actual forming process. A reciprocating tribometer set-up was technically designed to measure the high-resolution friction coefficient with a conformal contact configuration. The principal configuration of the test conformal pin-on-disc is shown in Fig. 5, of which the contact area between Al and test disc and the contact pressure is more accurately controlled than conventional point-contact ball-on-disc. A flat-end test pin made from AA6082-O (Ø 6 mm) was pressed against the plane surface of the bottom disc by a dead weight of 2-50 N. AA6082 pin was self-aligned with the disc to ensure the fully conformal contact. The disc made of tool material was reciprocating with a linear speed of 1 mm/s. The friction force at the tool/aluminium interface was measured by a torque sensor that is parallel to the sliding vector and the coefficient of friction (CoF) is calculated via the Coulomb friction law. The CoF is an average value around the periphery of Al-pin due to the symmetrical geometry of the tool.

Coating durability is another property that affects the tool life due to the fact that the tool was often due to repair as a result of die surface degradation. The durability of tooling can be indicated by the volume loss of material and it was tested on a standard ball-on-disc

tribometer (CSM® Ball-on-Disk). The testing procedure followed international standard ASTM G99. High temperature wear testing against AA6082 ball was carried out at 350 °C on the heated sample disc against aluminium alloy balls (Hv = 75). Comparative experiments were conducted using a hardened steel ball (HSS, Hv > 650) as a reference to the industrial universal testing procedure. Post-wear surface morphology was examined using interferometric profilometry integrated with the measurement of volume loss of the wear tracks.

3 Results and discussion

3.1 Performance of hot forming tools

Table 3 illustrates the parameters of test No.1-No.3 using the a-C DLC tool for stamping process. In order to eliminate the error from tool clearance and alignment, a comparison test named 'control' was performed on the tools using fully lubricated tools on both sides. After a series of testing using surface engineered blank-holders and inserts, the flange ratio ζ was measured according to Eq. (1). Fig. 6 gives the results of variation ζ and the change of the total flange length L_t (%). The control's ζ equals to 1 and its total length change L_t was 3% resulting from the plastic deformation of AA6082. It can be seen that when the 10 KN BHF was applied, the performance of coated tools did not match that of the lubricated untreated tool— ζ equals to 0.2 for sample lub/dry (C-10). However, when the BHF reduced to 5 KN, the coated side's performance was similar to the lubricated untreated side—ζ equals to 1.05 for sample lub/dry (C), indicating that the a-C treated stamping tools can be used to replace the lubricated tools at room temperature only with a small BHF.

A further development of tool coating was carried out and a WC: C coated tool was tested in hot and cold stamping conditions. Fig. 7 summarises the flange length variations ζ after

stamping, with the testing conditions presented in Table 4. The lubrication conditions on the WC: C tools were gradually reduced from 'Full' to '20% lub' or 'Dry', as a comparison to the fully lubricated tools on the left-side untreated die. At room temperature, the ζ remained within a range of 1.05-1.08 for the 'control' and test No. 2, which means that sample with 20% lubrication applied on WC: C coating provided a performance equivalent to the conventional lubrication. The best ratio was observed for No. 1 (WC: C tools plus full lubrication). The high ratio of ζ on sample lub/lub implies that a fully lubricated WC: C tools may provide better draw-ability than conventional tools thus it may be used to form more complex-shaped parts. This trend was also observed in hot stamping test conditions (test No. 5, 6 and 7)—a fully lubricated WC: C outperformed the left reference side demonstrated by a larger ζ (No. 5); on the other hand, stamping using 20% lubricant in hot conditions with such a WC: C coating technology (No.6) showed similar performance to that of the left-side fully lubricated untreated tool ($\zeta = 1$). From the above stamping test results, it can be concluded that the use of lubricant was largely reduced on the newly developed advanced surface engineering tools to obtain a performance similar to that of the fully lubricated untreated tool.

Fig. 8 shows the surface morphology and SEM micrographs of the insert surface retrieved from stamping. For the lubricated G3500 insert, there was a visible aluminium pick-up observed on the die radius of the insert. Another form of damage observed on the untreated G3500 cast iron was the prevalent pits which had the size of 0.1-0.5 mm across surface and corner caused by the corrosive hot lubricant (Fig. 8 (d)). In contrast, no pitting or general corrosion was observed on the WC: C tools, neither was it covered with much aluminium residue (Fig. 8 (e, f)). On the face area, a small amount of pick-up was found scattered around the edge of large graphite phase that exposed the graphite beneath the coating after stamping.

Nevertheless, WC: C tooling showed a reduced amount of the pick-up of aluminium especially in the corner area compared to the untreated G3500.

In order to analyse the stress distribution of the die, tension force along the tested blank is calculated using the following method. The material deformation of the top-hat stamping process can be assumed as a simplified plane strain stamping process which has a two-dimensional stress state. On a curved surface as seen in Fig. 2 (b) and Fig. 9 (a), the equilibrium tension T_1 in zone BC and DE with relation to pressure p and radius R can be expressed as:

$$T_1 = pR \tag{2}$$

On a small segment of arc (Fig. 2 (c)), there is a frictional shear stress μp, where μ is the coefficient of friction. The tension at the ends of this segment, point j and point k, can be calculated using Eq. (3):

$$\int_{T_{1j}}^{T_{1k}} \frac{dT_1}{T_1} = \int_0^{\theta_{jk}} \mu d\theta \tag{3}$$

where θ is the angle of wrap. The tensions at different positions are given as follows:

$$T_{1E} = T_{1D}\exp(-\mu\theta_{DE}) \tag{4}$$

$$T_{1C} = T_{1D} \tag{5}$$

$$T_{1A} = T_{1B} = 2\mu B \tag{6}$$

The tensions at different sections can be calculated using Eq. (3) to Eq. (6) because B in Eq. (6) is equal to the bank holding force used for drawing, and the corresponding pressure can be obtained using Eq. (2). Therefore, pressure distribution and tension force along the tested blank is calculated from Eqs. 4-6 and plotted in Fig. 9 (a). It can be seen that the

highest stress is mounted on the inner corner side of the die, which is more than double than the pressure on the face of die.

The pick-up rate at the different areas of the die is summarised in Fig. 9 (b). For both treated and untreated cast iron dies, an increased area of adhesion was recorded at the corner compared to the face area. This is probably due to the increasing contact pressure from 0.9 MPa (AB zone) to 2.3 MPa (BC and DE zone). Surface roughness is another important factor influencing the adhesion, where it showed in Fig. 9 (b) that the roughness at the corner is higher compared to that of face for both materials. This is believed to be caused by the non-uniform/wavy die surface resulted from the machining error. This roughness alteration perhaps also explains the uneven adhesion distribution phenomenon observed at the flange areas locally at the corner in Fig. 8 (a, b insert), where the two strips of concentrated adhesion zone at the two ends of the corner. After treating with WC: C, the adhesion rate on the corner is reduced to 8.5%, and notably the average roughness also decreased from 0.3 to 0.2, and 0.1 to 0.08, on the corner and face respectively. Thus, this study showed that the friction of aluminium on tooling is a complex phenomenon and takes different values depending on surface treatment, roughness R_a and pressure p. The effect of localised heat rising in the corner area to the adhesion of aluminium cannot be excluded, although it was not studied here. Based on above discussions, in order to prolong the lifetime of treated tools and allow the sheet to be drawn inwards without sticking to the tooling surface, lubrication on the high-stress areas especially die radius is recommended.

3.2 Tribology of treated cast iron tools

3.2.1 Dry sliding of AA6082 and cast iron

Figure 10 shows the friction between the AA6082 pin and cast iron G3500 treated varieties in relation to the number of sliding strokes. A contact pressure of 1.8 MPa equal with the top-

hat forming pressure was used in Fig. 10 (a). It shows that the CoF for the untreated G3500 tools and PN/PNC tools were very high (0.45) compared to that of the lubricated G3500 tools (0.1). Rising friction coefficient with service time phenomenon occurred as a result of the affinity between aluminium and tool material— an instant increase of CoF from the start of the test and levelled out over time. The CoF is controlled by two different components:

1) static friction coefficient at a constant pressure;

2) a pick-up contributing force during the repetitive sliding.

Therefore, the tested CoF can be expressed as follows:

$$\mu_i = \mu_s + \mu_0 \quad (7)$$

$$\mu_s = \sum_{i=0}^{n} K(S^n) \quad (8)$$

where μ_0 is the initial CoF tested at the start of pin-on-disc. μ_s is the correction component corresponding to the pick-up of sheet material. Eq. (8) was obtained through regression of the experimental results by IBM SPSS®. S is the number of strokes. μ_i is the CoF at a given time (i.e. strokes). Regarding the untreated tools, the initial friction force is small in the first couple of sliding cycles representing the geometric contact of surface asperities (i.e. CoF < 0.1 for G3500). With the onset of the aluminium transferring film, the contact pair changed from AA6082/tool to AA6082/AA6082 which results in the CoF increased progressively.

The interface CoF was greatly reduced when the tool was treated with advanced CAPVD coatings. The CoF of a-C coated tool was 0.17 in the first 5 cycles and it slowly reduced to 0.15, the CoF of a-C coated tools and WC: C coated cast iron tools remained low (0.15) for more than 20 cycles. A similar trend is also be observed in Fig. 10 (b) of which the CoF of various substrates was tested under the pressure of 0.07 MPa. The highest CoF was found on the untreated G3500 and PNC treated G3500, and the lowest CoF on carbonaceous varieties.

The CoF plots of the WC: C coating shows a clear trend of decreasing with the increasing cycles.

The dynamic CoF profiles of WC: C and a-C implicate a different mechanism on self-lubricated coatings compared to that of untreated G3500. The coated tools experience an underlining mechanism of material changes which exhibit interesting recession of friction coefficient over time. Carbon coating's 'friction recession' phenomenon was reported by IBM since the 1990s by Grill on DLC coatings (Grill 1999), suggesting that the free C bonds on the a-C film self-passivated when it contacted with the AA6082. The friction recession of DLC film depends greatly on the absorbance of hydrogen molecule on the contacting interface as reported by (Konca et al. 2007). Hydrogenated DLC film can work in an H^+-absence environment whereas non-H DLC must work through the bonding of the C atoms with the H from the atmosphere. As the WC: C and a-C prepared in this study are both non-H carbonaceous coatings, they passivated though the surface absorption of H from the interface molecules during sliding. In addition, the structured transformation from DLC to sp2 C at the superficial layer, and the transfer of this layer of C to the counterpart contributing to a C-C contact couple was also discussed in (Erdemir et al. 1995) and might contribute to the reducing coefficient of the WC: C coating found in this study.

These tribology results reflect the similar trends obtained from the deep-drawing trials. The interfacial friction coefficient is decreased by coating technologies which allow test-piece material to be drawn into the die as shown in sample lub/20% (test No.2) in Fig. 7. It also demonstrates that the WC: C provide a relative lower CoF compared to other solid lubricant coatings previously developed such as MoS_2 (Sivarajan et al. 2014), VC (Sugimoto 1989), Si_3N_4 and oxide ceramics (Kataoka et al. 2004). The coefficient of friction is an important input parameter for the finite simulation analysis and modelling of tooling design for the

forming process. It is relatively easier to predict the increasing CoF for uncoated G3500 compared to the reverse phenomenon on the surface of WC: C coated tools. It was suggested by Shimizu et al. (Shimizu et al.) that a surface roughness model integrated FE analysis might be used to pick up the effect of surface asperities. However, the result in this study shows that it is difficult to observe interface phenomena and build a vigorous model for adhesion-friction behaviour as found in forming of aluminium.

3.2.2 Durability of coated HFQ® tool

The service lifetime of forming tool depends largely on its durability; for aluminium stamping, it can be indicated by the materials' wear rate against aluminium alloy. The wear rates related to the tool hardness and the adhesion rate are shown in Fig. 11. By comparison of Figures 11 (a) and (b), The wear rate of untreated G3500 tool material was very high ($1.3x10^{-5}$ mm^3/Nm, HSS ball) due to its low hardness (3.3 GPa). Wear rate decreased to $2.6x10^{-7}$ mm^3/Nm on the surface of a-C coated tools of which the hardness was 16 GPa. In addition, coatings with lower adhesion rate also demonstrate lower CoF. For WC: C coated tool, the hardness was 5.2 GPa— significantly lower than that of a-C—but the wear rate of WC: C was also low ($4.7x10^{-7}$ mm^3/Nm, HSS ball). This is attributed to the fact that the WC: C has the lowest adhesion rate among all materials (10^{-14} m^3/Nm). Accordingly, the CoF dropped to 0.1-0.15 and the wear dropped to $1.5x10^{-6}$ mm^3/Nm against aluminium, which suggests that the lower wear rate prevailed at either the higher hardness of the material or the ones with lower adhesion rate.

Post-wear surface morphology (Fig. 12) revealed that the AA 6082 transfer occurred from a very small contact area on the untreated tool, rather than uniformly covering the contact surface, indicating that the building up of the aluminium involves repetitive bonding and breaking of Al-on-Al asperities. Lubricity between tool and aluminium affects the wear resistance to a great extent—the specimens coated with WC: C was relatively free from

adhesion and no severe damage of the coatings was observed. At the surface of WC: C treated tool, two contacted surfaces were separated by the carbon solid lubricant thus the metal transfer was reduced. As suggested by Nouari (Nouari et al. 2003) that the aluminium adhesion-bonding mechanism at elevated temperature plays a vital role in the dry machining of aluminium. This work addresses the phenomenon of tribology at high temperature for aluminium forming, and the available data has been obtained specifically from a practice of deep drawing of aluminium. Hence, using surface engineered cast iron tools in the industrial stamping process was suggested to save the consumption of lubricant and cost of tools, in order to form AA6082 component with light weight and great geometry complexity.

4 Conclusions

The hot-metal-forming performance of advanced surface engineered forming tools was tested against the AA6082 alloys using the lubricated cast iron as a reference. A newly constructed top-hat experiment rig was employed for cold and hot stamping tests. The results showed that at room temperature, the dry forming of AA6082 on an a-C DLC coated tools failed by using 10 KN blank-holding force, however, succeeded after decreasing the blank-holding force to 5 KN. Hot stamping using WC: C coated tool succeeded to produce a drawing depth of 70 mm by using only 20% amount of lubricant, however, failed when lubricant was entirely removed and stamping in the dry condition. When the tools were fully hydro-lubricated, the WC: C out-performed the lubricated untreated G3500 during both cold and hot stamping, which indicates the potential use of the WC: C coated tools for the forming of complex AA6082 shapes. The tested friction coefficient was also reduced from 0.5 to 0.15 by applying WC: C; and the wear rate of forming tools can be reduced by 5 times using the selected surface treatment of plasma nitrocaburising. During forming, a significant reduction of aluminium adhesion was observed on the WC: C coated tools than on the other tested tool

materials. Due to the stress concentration existing at the corner of tools, a small amount of lubricant applied at the local die corner area is recommended to avoid adhesion phenomenon.

5 Acknowledgement

The authors gratefully acknowledge the financial support of the EU FP7 LoCoLite project (Contract No GA604240). Appreciation also is extended to the S.C. Plasmaterm S.A. Romania for the supply of castings and machining. HFQ® is a registered trademark of Impression Technologies Ltd.

References

K. Agarwal, R. Shivpuri, J. Vincent, E. Rolinski, G. Sharp
2013 DC pulsed plasma deposition of nanocomposite coatings for improved tribology of gray cast iron stamping dies. J. Mater. Process. Technol. 213, pp. 864-876 http://dx.doi.org/10.1016/j.jmatprotec.2013.01.002

A. Aginagalde, X. Gomez, L. Galdos, C. García
2009 Heat Treatment Selection and Forming Strategies for 6082 Aluminum Alloy. J. Eng. Mater. Technol. 131, pp. 044501 doi: 10.1115/1.3120384

S. Bhowmick, A.T. Alpas
2008 The performance of hydrogenated and non-hydrogenated diamond-like carbon tool coatings during the dry drilling of 319 Al. International Journal of Machine Tools and Manufacture 48, pp. 802-814 http://dx.doi.org/10.1016/j.ijmachtools.2007.12.006

D.H. Buckley
1975 Wear and interfacial transport of material. Journal of Vacuum Science & Technology 13, pp. 88-95 doi:http://dx.doi.org/10.1116/1.568963

K. Dohda, T. Aizawa
2014 Tribo-characterization of silicon doped and nano-structured DLC coatings by metal forming simulators. Manufacturing Letters 2, pp. 82-85 http://dx.doi.org/10.1016/j.mfglet.2014.03.001

Y. Dong, D. Formosa, J. Fernandez, X. Li, G. Fuentes, K. Zoltan, H. Dong
2015 Development of low-friction and wear-resistant surfaces for low-cost Al hot stamping tools. MATEC Web of Conferences 21, pp. 05009 http://dx.doi.org/10.1051/matecconf/20152105009

A. Erdemir, C. Bindal, J. Pagan, P. Wilbur
1995 Characterization of transfer layers on steel surfaces sliding against diamond-like hydrocarbon films in dry nitrogen. Surf. Coat. Technol. 76–77, Part 2, pp. 559-563 http://dx.doi.org/10.1016/0257-8972(95)02518-9

H. Fukui, J. Okida, N. Omori, H. Moriguchi, K. Tsuda
2004 Cutting performance of DLC coated tools in dry machining aluminum alloys. Surf. Coat. Technol. 187, pp. 70-76 doi: 10.1016/j.surfcoat.2004.01.014

A. Grill
1999 Diamond-like carbon: state of the art. DRM 8, pp. 428-434 http://dx.doi.org/10.1016/S0925-9635(98)00262-3

M.D. Hanna
2009 Tribological evaluation of aluminum and magnesium sheet forming at high temperatures. Wear 267, pp. 1046-1050 http://dx.doi.org/10.1016/j.wear.2009.01.007
B.G. Hansen, N. Bay
1986 Two new methods for testing lubricants for cold forging. Journal of Mechanical Working Technology 13, pp. 189-204 http://dx.doi.org/10.1016/0378-3804(86)90065-3
J. Heinrichs, M. Olsson, S. Jacobson
2012 Mechanisms of material transfer studied in situ in the SEM:: Explanations to the success of DLC coated tools in aluminium forming. Wear 292–293, pp. 49-60 http://dx.doi.org/10.1016/j.wear.2012.05.033
S. Kataoka, M. Murakawa, T. Aizawa, H. Ike
2004 Tribology of dry deep-drawing of various metal sheets with use of ceramics tools. Surf. Coat. Technol. 177-178, pp. 582-590 doi: 10.1016/S0257-8972(03)00930-7
E. Konca, Y.T. Cheng, A.M. Weiner, J.M. Dasch, A.T. Alpas
2007 The Role of Hydrogen Atmosphere on the Tribological Behavior of Non-Hydrogenated DLC Coatings against Aluminum. Tribology Transactions 50, pp. 178-186 doi: 10.1080/10402000701260906
P.E. Krajewski, A.T. Morales
2004 Tribological issues during quick plastic forming. J. Mater. Eng. Perform. 13, pp. 700-709 doi: 10.1361/10599490421330
H. Laurent
2007 FALET-HL-CEMUC–Forming of aluminum alloys at elevated temperature. European Commission 220688, pp. 1-5
A. Mihail, M. Rodzik
2007 Design and Manufacturing a DP980 B-Pillar Inner for the GM Chevy Equinox / Pontiac Torrent. Great designs in steel pp. 23
M. Murakawa, N. Koga, T. Kumagai
1995 Deep-drawing of aluminum sheets without lubricant by use of diamond-like carbon coated dies. Surf. Coat. Technol. 76–77, Part 2, pp. 553-558 http://dx.doi.org/10.1016/0257-8972(95)02523-5
M. Murakawa, S. Takeuchi
2003 Evaluation of tribological properties of DLC films used in sheet forming of aluminum sheet. Surf. Coat. Technol. 163–164, pp. 561-565 http://dx.doi.org/10.1016/S0257-8972(02)00624-2
M. Nouari, G. List, F. Girot, D. Coupard
2003 Experimental analysis and optimisation of tool wear in dry machining of aluminium alloys. Wear 255, pp. 1359-1368 doi: 10.1016/S0043-1648(03)00105-4
E. Rolinski
1987 Effect of plasma nitriding temperature on surface properties of austenitic stainless steel. Surf. Eng. 3, pp. 35-40 doi: 10.1179/sur.1987.3.1.35
E. Roliński, A. Konieczny, G. Sharp
2009 Nature of surface changes in stamping tools of gray and ductile cast iron during gas and plasma nitrocarburizing. J. Mater. Eng. Perform. 18, pp. 7 doi: 10.1007/s11665-009-9352-7
T. Shimizu, M. Yang, K.-i. Manabe
Impact of Surface Topography of Tools and Materials in Micro-Sheet Metal Forming, Metal Forming - Process, Tools, Design. In: M. Kazeminezhad, Metal Forming - Process, Tools, Design,
S. Sivarajan, R. Padmanabhan
2014 Green Machining and Forming by the use of Surface coated tools. Procedia Engineering 97, pp. 15-21 http://dx.doi.org/10.1016/j.proeng.2014.12.219

M. Sugimoto
1989 Recent development of sheet metal press forming in Japan. International Journal of Machine Tools and Manufacture 29, pp. 39-53 http://dx.doi.org/10.1016/0890-6955(89)90053-9
K. Uda, A. Azushima, A. Yanagida
2016 Development of new lubricants for hot stamping of Al-coated 22MnB5 steel. J. Mater. Process. Technol. 228, pp. 112-116 http://dx.doi.org/10.1016/j.jmatprotec.2015.10.033
F. Vollertsen, H. Flosky, T. Seefeld
2015 Dry metal forming - a green approach. In: A.E. Tekkaya, H. Werner and B. Alexander (eds.), 60 Excellent Inventions in Metal Forming, pp. 113-118
A. Wank, G. Reisel, B. Wielage
2006 Behavior of DLC coatings in lubricant free cold massive forming of aluminum. Surf. Coat. Technol. 201, pp. 822-827 http://dx.doi.org/10.1016/j.surfcoat.2005.12.043

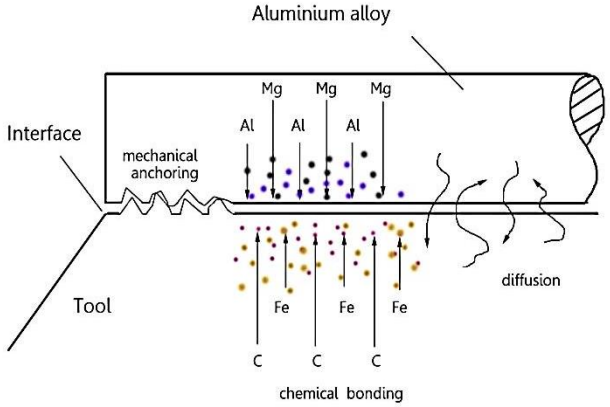

Fig. 1. A schematic diagram of the adhesion between aluminium alloy and iron.

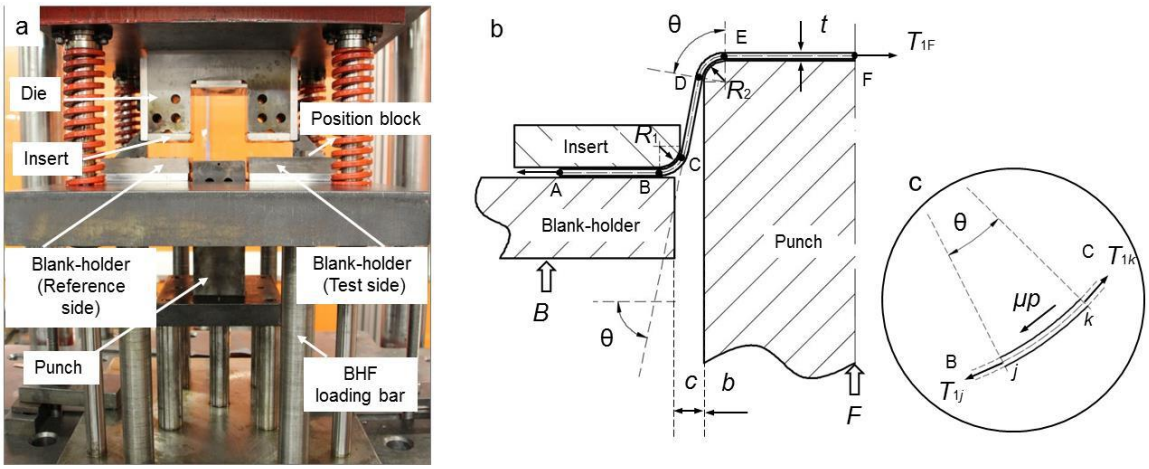

Fig. 2. Setup of the top-hat stamping test rig: (a) loading cell containing test dies and reference dies (b) schematic diagram of top-hat part forming; (c) a small segment of arc within zone BC.

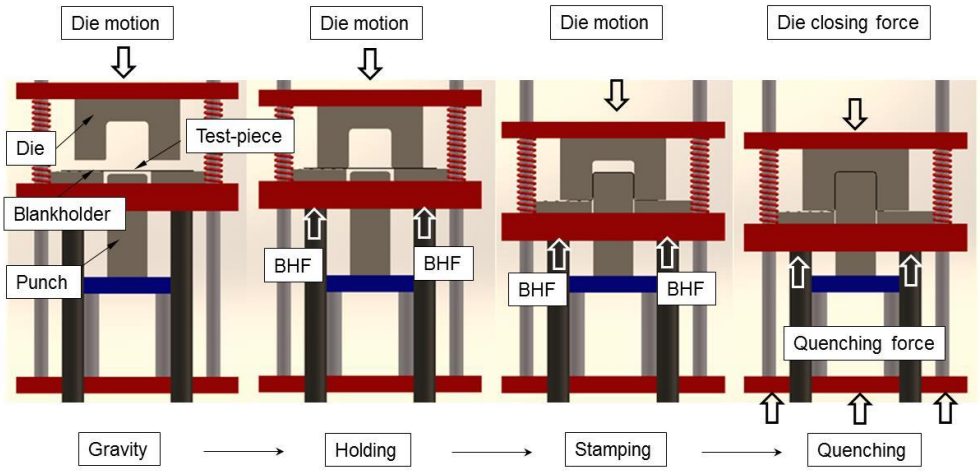

Fig. 3. Stages of motion of top-hat parts forming with controllable BHF.

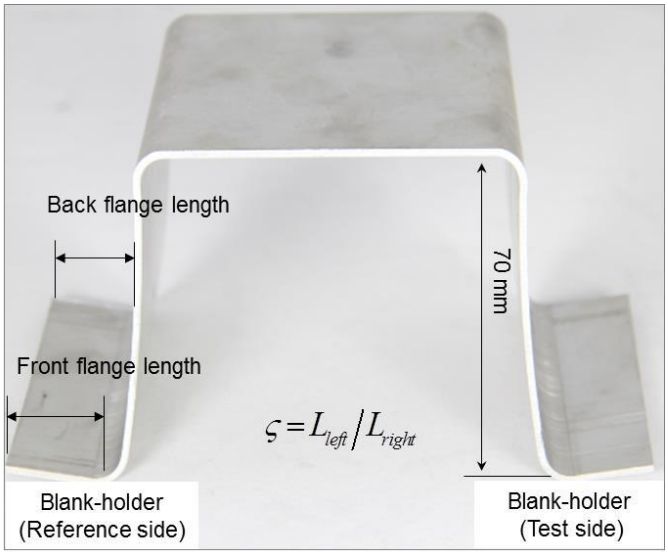

Fig. 4. Formed part with the definition of flange length ratio ζ.

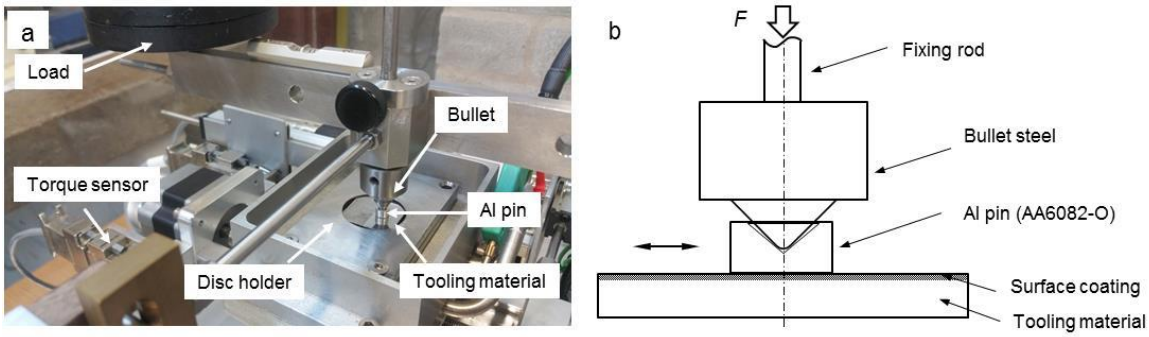

Fig. 5. (a) Principal configuration of the reciprocating pin-on-disc under a constant load, and (b) the self-aligned conformal contact between pin and tested tooling material.

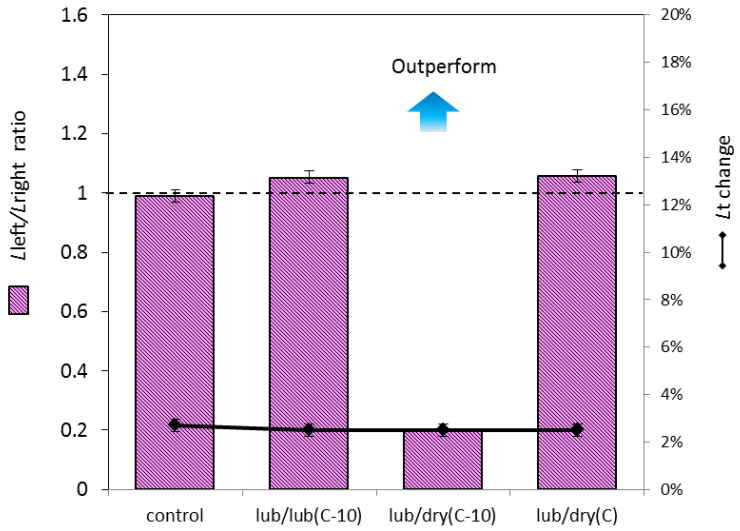

Fig. 6. Assessment of L_{left}/L_{right} and L_t of top-hat parts using a-C coated tools as compared to the conventional lubricated tools, BHF=5kN, 10kN, T=20°C.

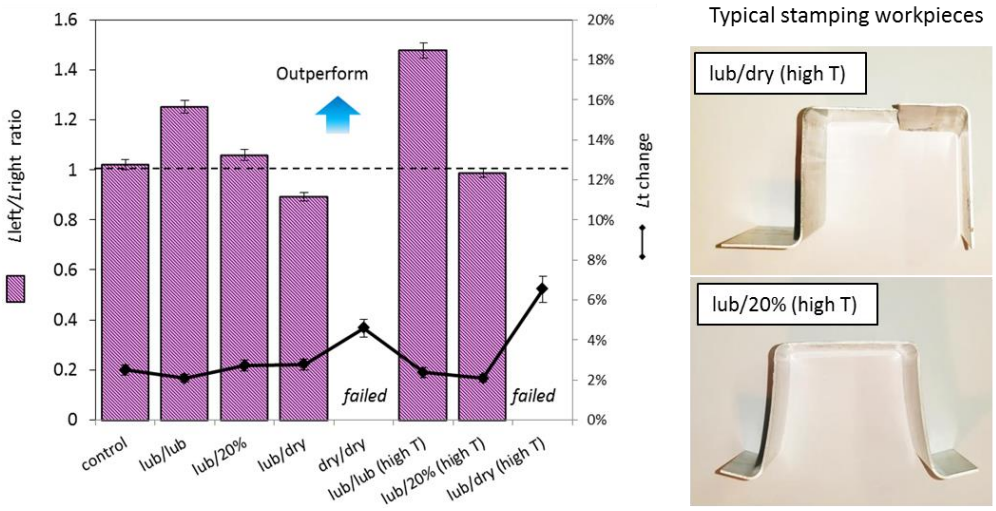

Fig. 7. Assessment of L_{left}/L_{right} and L_t of top-hat parts forming using WC: C coated tools at BHF=5kN, T=20°C, 430°C.

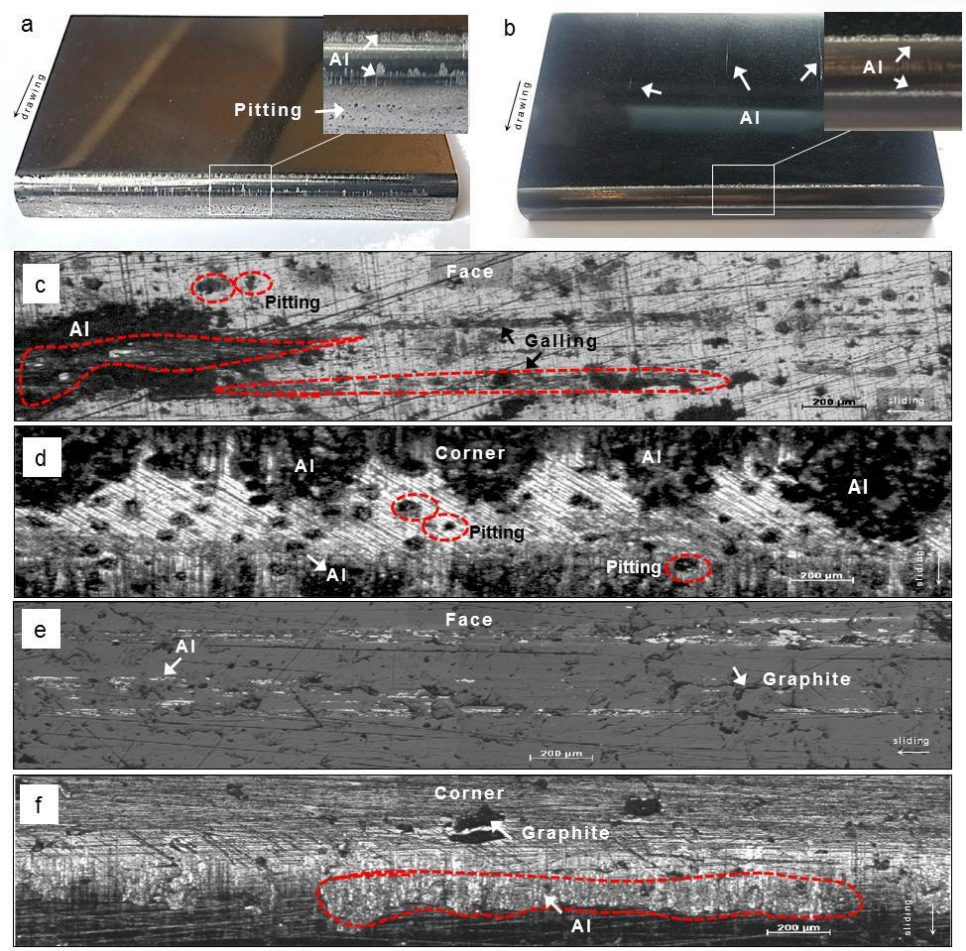

Fig. 8. Surface morphology of the insert showing the aluminium transfer and corrosion of die surface. Note the drawing directions indicated by the arrows, (a, c, d) G3500 and (b, e, f) CAPVD WC: C treated cast iron.

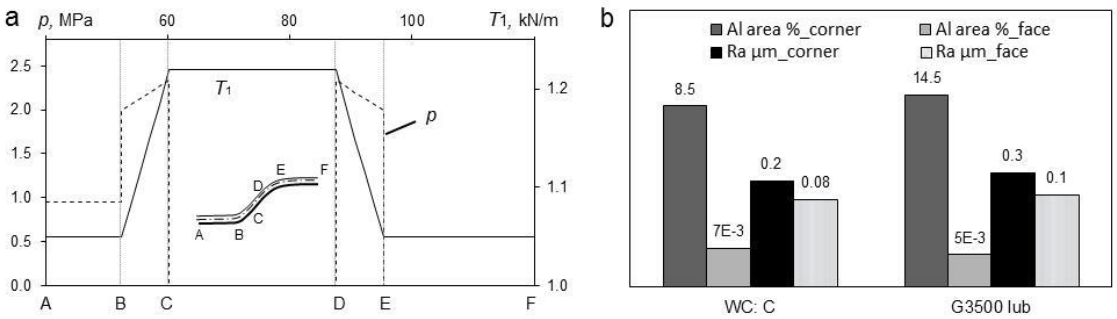

Fig. 9. (a) Pressure and tension distribution along the deformed sheet based on simplified plane strain stamping model, and (b) average adhesion rate on the tooling areas and its average roughness *R*a prior to stamping.

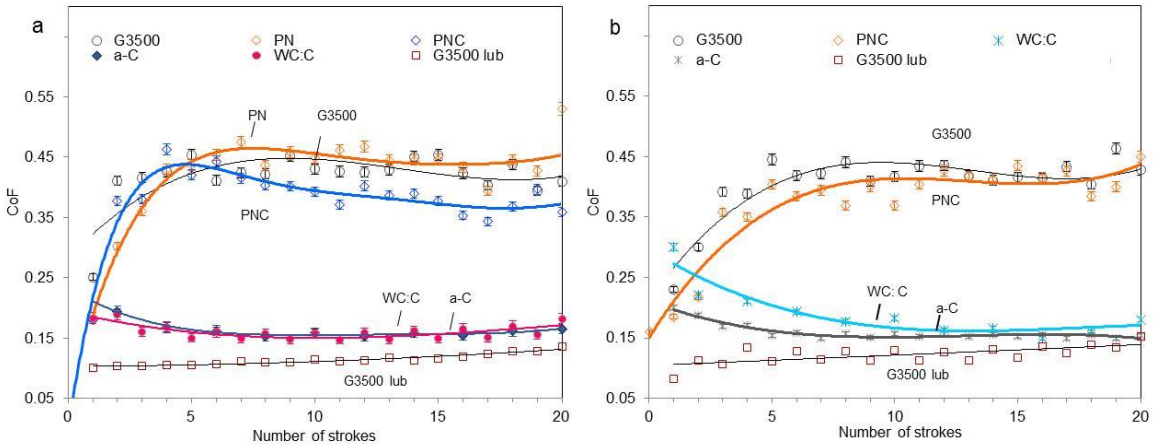

Fig. 10. The polynomial fitting of CoF (±SD) of coated and uncoated stamping tools used for HFQ® AA 6082 sheet, (a) pressure = 1.8 MPa, (b) pressure = 0.07 MPa.

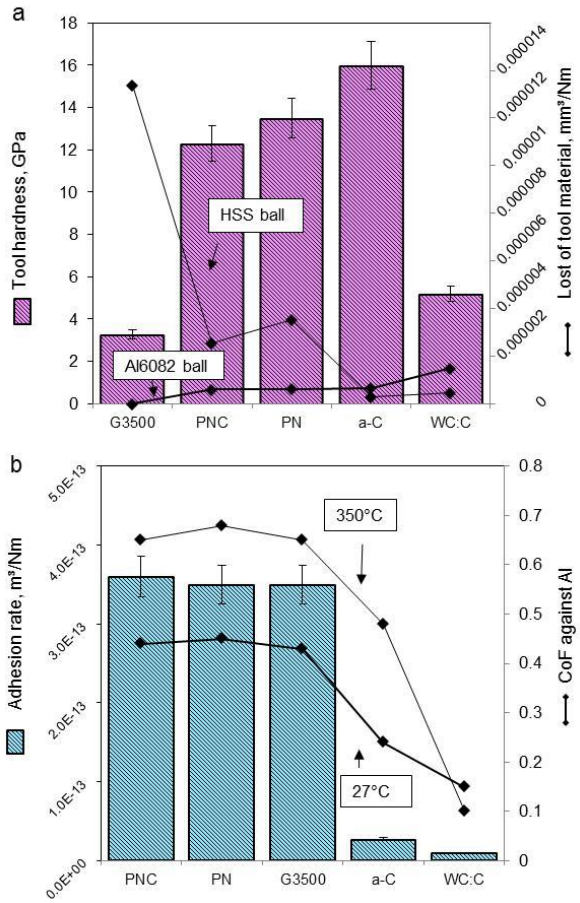

Fig. 11. (a) Mean wear rates of the HFQ® stamping tools at 350 °C with correlation to the coating hardness, and (b) the adhesion rate of AA6082 at 350 °C with correlation to the friction coefficient of AA6082.

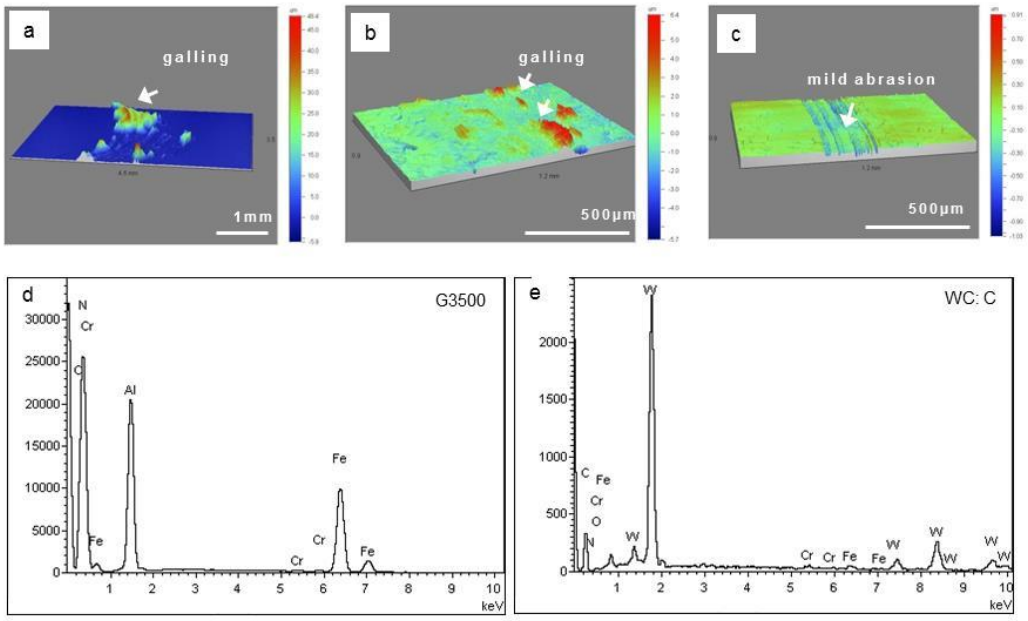

Fig. 12. Wear scars on various (a) G3500, (b) PNC and (c) WC: C coated tooling surface and post-wear EDS on (d) G3500 and (e) WC: C, condition: Al balls AA6082, 350 °C, 2 N, and 500 cycles.

Table 1. Chemical composition of AA6082

Element	Mn	Fe	Mg	Si	Cu	Zn	Ti	Cr	Al
wt %	0.4-1.0	<0.5	0.6-1.2	0.7-1.3	<0.1	<0.2	<0.1	<0.25	Balance

Table 2. Blank and die parameters of top hat drawing

Blank and die geometries		Process parameters	
Blank size:	240×86×1.5 mm	Blank-holding force:B:	5-10 kN
Side clearance: c	1.65 mm	Quenching force:	20 kN
Punch semi-width: b	36 mm	Forming speed:	150 mm/s
Die/Punch corner radius: R_1 and R_2	5 mm	Die holding time:	10 s

Table 3. The forming conditions of HFQ® AA6082 using tool materials coated with a-C DLC

No.	Sample label (left/right)	Blank T. (°C)	Lubrication conditions		Tooling conditions		BHF (KN)
			Left	Right	Left	Right	
	control	20°C	Full	Full	Un-treated	Un-treated	10
1	lub/lub(C-10)	20°C	Full	Full	Un-treated	a-C DLC	10
2	lub/dry(C-10)	20°C	Full	Dry	Un-treated	a-C DLC	10
3	lub/dry(C)	20°C	Full	Dry	Un-treated	a-C DLC	5

Table 4. The forming conditions of HFQ® AA6082 using tool materials coated with WC: C

No.	Sample label (left/right)	Blank T. (°C)	Tooling conditions		Lubrication condition		BHF (KN)
			Left	Right	Left	Right	
	control	20°C	Un-treated	Un-treated	Full	Full	10
1	lub/lub	20	Un-treated	WC: C	Full	Full	5
2	lub/20%	20	Un-treated	WC: C	Full	20% lubricated	5
3	lub/dry	20	Un-treated	WC: C	Full	Dry	5
4	dry/dry	20	Un-treated	WC: C	Dry	Dry	5
5	lub/lub (high T)	430	Un-treated	WC: C	Full	Full	5
6	lub/20% (high T)	430	Un-treated	WC: C	Full	20% lubricated	5
7	lub/dry (high T)	430	Un-treated	WC: C	Full	Dry	5